



# Vision-based Control of the Mixing-Layer

D. Anda Ondo , C. Collewet , J. Carlier 

 **irstea Rennes, TERE - ACTA**  
 INRIA, Fluminance

GDR CDD-MOSAR, LIMSI, Orsay, 17/11/2014

# Outline

- 1 Introduction
- 2 The choice of the control
- 3 The modelling
- 4 The First results
- 5 Conclusion

## Context: climate separation in food industry (1/2)

More than half of food purchases are perishable products presented for sale in cold environment.

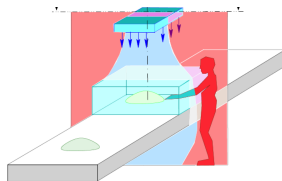


Figure 1: Climate separation device Froiloc© developed by Irstea

⇒ The emergence of new techniques comes from the need to address the contradiction between the **food safety objective** of maintaining cold environments, possibly ultra-clean, and **work conditions objective** of raising the temperature of the environment experienced by operators.

## Context: climate separation in food industry (2/2)

These techniques aim to improve:

- food safety;
- work conditions;
- energy saving.

The climate separation devices are developed and optimized in stabilized conditions, but confronted to the industrial environments, **these devices see their performances of separation deteriorated.**

⇒ **Our motivation is to improve the climate separation with a closed-loop control.**

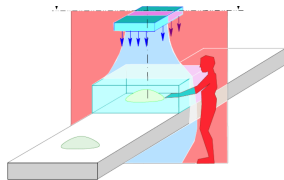


**Figure 1:** Climate separation device Froiloc© developed by Irstea

## Context: climate separation in food industry (2/2)

These techniques aim to improve:

- food safety;
- work conditions;
- energy saving.

The climate separation devices are developed and optimized in stabilized conditions, but confronted to the industrial environments, **these devices see their performances of separation deteriorated.**

⇒ **Our motivation is to improve the climate separation with a closed-loop control.**

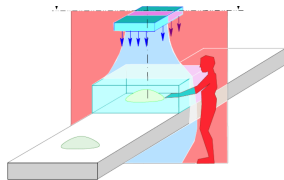


**Figure 1:** Climate separation device Froiloc© developed by Irstea

## The mixing layer (1/2)

In new climate separation techniques (see Fig. 1), interfaces between the two environments (blue and red) can be modeled by a typical mixing-layer.

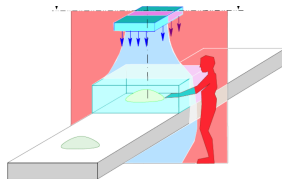


**Figure 1:** Climate separation device Froiloc© developed by Irstea

In the mixing-layer, the flow is turbulent (see Fig. 2).

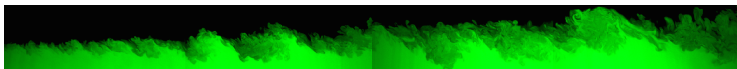


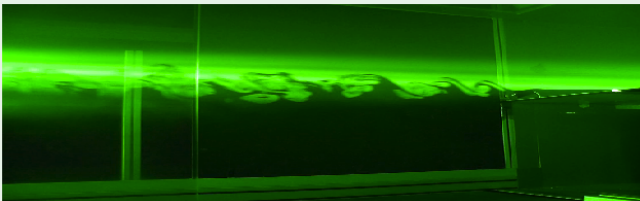
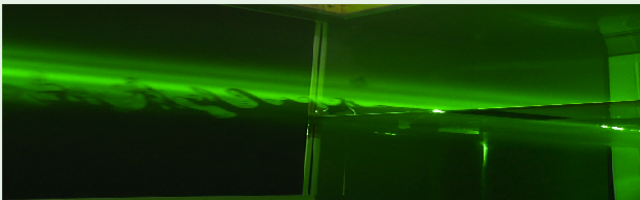
**Figure 2:** Visualisation of the mixing-layer in the wind tunnel of Irstea

## The mixing layer (2/2)

There is a considerable bibliography on the Mixing-Layer, whose the main subjects are:

- analysis stability, see e.g. (Michalke, 1964, Ho and Huerre, 1984);
- mean behaviour in self similarity regions, see e.g. (Wygnanski and Fiedler (1970), ☺ Sadjavi and Carlier (2013));
- forcing or open loop-control, see e.g. (Oster and Wygnanski, 1982, Ho and Huang, 1982, Koochesfahani and MacKinnon, 1991);
- closed-loop control, recently, see e.g. (Wiltse and Glezer, 2011, Parezanovic et al., 2014). Others turbulent systems, see e.g. (Gautier and Aider, 2014, Duriez et al., 2013).

## Visualisation of the forced mixing-layer of the wind tunnel



(Chatelain et al., 2013).



# Outline

- 1 Introduction
- 2 The choice of the control
- 3 The modelling
- 4 The First results
- 5 Conclusion

# Outline

- 1 Introduction
- 2 The choice of the control
- 3 The modelling
- 4 The First results
- 5 Conclusion

# The control?

We use closed-loop control: depends of an observation of the system.

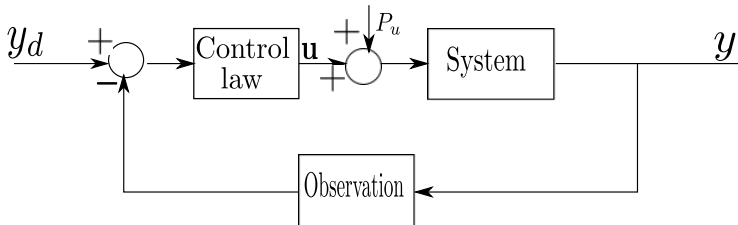


Figure 3: Closed-loop control of a disturbed system

## Advantages:

- Robustness to the modeling errors;
- robustness to the disturbances on the system.

# The vision-based control (1/2)

## The sensor: Camera

### Advantages:

- is accurate for the state estimation;
- offers a large choice of desired states (base flow → unsteady flow);
- can be used to get a dynamical model of the desired state.

### Limits?

- real-time processing;
- visualisation of the flow.

## Usual domains of use

- robotics (industrial, medical, mobile or motion);
- augmented reality, computer animation,.. (more limited degree)
- and more recently, in flow control.



## The vision-based control (2/2)

- Goal: closed-loop control of flow fluid;
- Display device
  - extract the  $2D$  velocity field by optical flow;
  - choice of the visual informations
- modelling of the variation of visual informations depending of variation of control signal: computation of the interaction matrix;
- synthesis of the control law;
- actuation on the fluid flow.

(Tatsambon Fomena and Collewet, 2011, Dao and Collewet, 2012, Roca et al., 2014, Gautier and Aider, 2014)

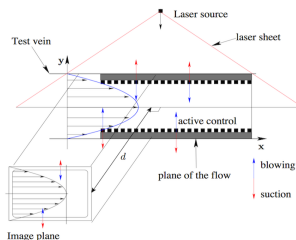


Figure 4: Example of use of vision in control of Poiseuille flow

# Outline

- 1 Introduction
- 2 The choice of the control
- 3 The modelling**
- 4 The First results
- 5 Conclusion

# Design of the state space model (1/4)

Let consider Navier-Stokes equations on incompressible flow

$$\partial_t \vec{U} + (\vec{U} \cdot \nabla) \vec{U} = -\frac{1}{\rho} \nabla P + \nu \Delta \vec{U} \quad (1a)$$

$$\nabla \cdot \vec{U} = 0. \quad (1b)$$

We consider also flow around a given profile  $\vec{U}_b$  such that  $\partial_t \vec{U}_b = 0$  and

$$(\vec{U}_b \cdot \nabla) \vec{U}_b = -\frac{1}{\rho} \nabla P + \nu \Delta \vec{U}_b. \quad (2)$$

These fields verify the continuity equation

$$\nabla \cdot \vec{U}_b = 0. \quad (3)$$

After some computations (**linearisation, dimensionless**), we can write

$$\mathcal{L} \dot{X} = AX + BU. \quad (4)$$

$\mathcal{L}$  is not invertible matrix!

## Design of the state space model (2/4)

To write the system (1) with the classical form

$$\dot{\mathcal{X}} = A\mathcal{X} + BU, \quad (5)$$

we use representations which allow to re-write the system (1) with two variables: **vorticity/stream-function** and **velocity/vorticity**.

In the case of vorticity/stream-function formulation, we use the stream-function  $\psi(x, y, t)$  such that

$$u = \partial_y \psi, \quad (6)$$

$$v = -\partial_x \psi, \quad (7)$$

$$\omega_z = -\nabla^2 \psi. \quad (8)$$

And finally, we can express the Navier-Stokes equations only with the stream-function

$$\left[ (\partial_t + U_b \partial_x) \Delta - \partial_y^2 U_b \partial_x - \frac{1}{Re} \Delta^2 \right] \psi = 0. \quad (9)$$



## Design of the state space model (3/4)

The boundary conditions are

- $\partial_y \vec{u}(x, y = 0, t) = 0;$
- $\partial_y \vec{u}(x, y = 1, t) = 0;$
- $\partial_x \vec{u}(x = 1, y, t) = 0;$
- $\vec{u}(x = 0, y, t) = \mathbf{u}.$

Using simple semi-discrete formulation (finite differences in space), we can write

$$\mathbb{L}\partial_t[\psi](t) = \mathbb{A}[\psi](t) \quad (10)$$

where  $\mathbb{L}$  is an invertible matrix and  $[\psi]$  is the vector representing the set of considered stream-function.

We can then express an autonomous system given by

$$\partial_t[\psi] = \mathbb{L}^{-1}\mathbb{A}[\psi] = \mathcal{A}[\psi] \quad (11)$$

## Design of the state space model (3/4)

The boundary conditions are

- $\partial_y \vec{u}(x, y = 0, t) = 0;$
- $\partial_y \vec{u}(x, y = 1, t) = 0;$
- $\partial_x \vec{u}(x = 1, y, t) = 0;$
- $\vec{u}(x = 0, y, t) = \mathbf{u}.$

Using simple semi-discrete formulation (finite differences in space), we can write

$$\mathbb{L}\partial_t[\psi](t) = \mathbb{A}[\psi](t) \quad (10)$$

where  $\mathbb{L}$  is an invertible matrix and  $[\psi]$  is the vector representing the set of considered stream-function.

We can then express an autonomous system given by

$$\partial_t[\psi] = \mathbb{L}^{-1}\mathbb{A}[\psi] = \mathcal{A}[\psi] \quad (11)$$

## Design of the state space model (4/4)

Now we need to differency the control space and the state space to be controlled.

There exist matrices  $M$  and  $M_c$ , with appropriate dimensions, such that we have

$$[\psi] = M[\psi]_r + M_c[\psi]_u, \quad (12)$$

and such that we have  $M^T M = \mathbb{I}$ ,  $M^T M_c = 0$ , ([Anda Ondo, 2013](#)).

Using (12), we have

$$\begin{aligned} M^T M \partial_t [\psi]_r &= M^T \mathcal{A} M [\psi]_r + M^T \mathcal{A} M_c [\psi]_u - M^T M_c \partial_t [\psi]_u \\ \Leftrightarrow \partial_t [\psi]_r &= M^T \mathcal{A} M [\psi]_r + M^T \mathcal{A} M_c [\psi]_u \end{aligned} \quad (13)$$

So we can express our controlled state space such that

$$\dot{\mathcal{X}} = A\mathcal{X} + BU. \quad (14)$$

# On the controllability of the obtained models (1/2)

Let consider the system

$$\dot{\mathcal{X}} = A\mathcal{X} + BU, \quad (15)$$

before we compute a control law, we have to verify that our model is controllable. The following assertions are equivalent:

- the pair  $(A, B)$  is stabilizable;
- there exists a matrix  $\mathcal{K}$  such that  $(A + B\mathcal{K})$  is stable;
- using the Popov-Belevitch-Hautus criterion (or PBH):  
 $\text{rank}([A - \lambda\mathbb{I} \quad B]) = nx \cdot ny \quad \forall \lambda \in \text{spec}(A) \cap \mathbb{C}_+^*$ .

Using the PBH criterion, we test the controllability of the system for  $nx$  and  $ny$  such that

$$nx = ny \in (4 \quad 8 \quad 12 \quad 16 \quad 20) \quad (16)$$

# On the controllability of the obtained models (2/2)

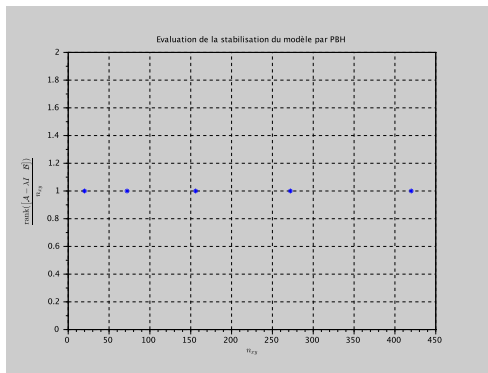


**Figure 5:** Stabilizability of the model: for each given  $n_{xy}$ , all real positive eigenvalues of  $A$  are tested. The minor rank is then divided by  $n_{xy}$ .

## The Linear Quadratic Regulator (LQR) (1/2)

The problem of the control LQR is resolved using the closed-loop control which minimizes the functional cost

$$\int_0^{\infty} (\mathcal{X}^T(t) \mathcal{Q} \mathcal{X}(t) + \mathcal{U}^T(t) \mathcal{R} \mathcal{U}(t)) dt \quad (17)$$

where  $\mathcal{Q} = \mathcal{Q}^T \geq 0$  and  $\mathcal{R} = \mathcal{R} > 0$ ,  $\mathcal{U} = -\mathcal{K} \mathcal{X}$  with  $\mathcal{K} = \mathcal{R}^{-1} B^T \mathcal{P}$  and  $\mathcal{P} = \mathcal{P}^T$  is the solution of the algebraic Riccati equation

$$A^T \mathcal{P} + \mathcal{P} A - \mathcal{P} B \mathcal{R}^{-1} B^T \mathcal{P} + \mathcal{Q} = 0. \quad (18)$$

How to determine  $\mathcal{Q}$  and  $\mathcal{R}$  in the case of the mixing-layer?

Matrices  $\mathcal{Q}$  is given such that, (M<sup>c</sup>Kernan, 2006):

$$\mathcal{X}^T \mathcal{Q} \mathcal{X} = E = \frac{1}{V} \int_V \rho \frac{\vec{u}^T \vec{u}}{2} dV \quad (19)$$

where  $E$  is the unitary volume energy.

## The Linear Quadratic Regulator (LQR) (2/2)

Using the discrete approximation of (19), we have, after some computations,

$$\begin{aligned}
 \mathcal{X}^T \mathcal{Q} \mathcal{X} \simeq & \quad dx dy \sum_{j=0}^{ny} \left( \frac{1}{4dx^2} \begin{bmatrix} \psi_{i=0, \dots, nx-1}^2 \\ 0 \end{bmatrix}_j + \frac{1}{4dx^2} \begin{bmatrix} 0 \\ \psi_{i=1, \dots, nx}^2 \end{bmatrix}_j \right. \\
 & \quad + \frac{1}{4dy^2} \begin{bmatrix} \psi_i^2 \end{bmatrix}_{j-1} + \frac{1}{4dy^2} \begin{bmatrix} \psi_i^2 \end{bmatrix}_{j+1} \\
 & \quad \left. - \frac{2}{4dx^2} \begin{bmatrix} 0 \\ \psi_{i+1} \psi_{i-1} \\ 0 \end{bmatrix}_j - \frac{2}{4dy^2} [\psi_i]_{j+1}^T [\psi_i]_{j-1} \right), \quad (20)
 \end{aligned}$$

where we assume the length in  $z$ -direction is 1.

The matrix  $\mathcal{R}$  can be defined such that

$$\mathcal{R} = r^2 \mathbb{I}. \quad (21)$$

# Outline

- 1 Introduction
- 2 The choice of the control
- 3 The modelling
- 4 The First results**
- 5 Conclusion



# Incompact3D: a real-like system (1/2)

*Incompact3D is a powerful numerical tool for academic research. It can combine the versatility of industrial codes with the accuracy of spectral codes, see (Laizet and Lamballais, 2011).*

<https://code.google.com/p/incompact3d/>

## Advantages:

- based on a cartesian mesh (allow to implement high order compact schemes);
- Immersed Boundary Method;
- Poisson equation is fully solved in spectral space;
- large choice of boundary conditions.

## Incompact3D: a real-like system (2/2)

Simulation of the mixing-layer with upstream Strouhal frequency excitation.

## Results: the simulation scenario

The Incompact3D is implemented with the following parameters:

- The box is such that:  $n_x = 512$ ,  $n_y = 256$  and  $n_z = 8$ ;
- Reynolds number:  $Re = 300$ ;
- velocities:  $u_{high} = 2$  and  $u_{low} = 1$ ;
- Boundary conditions such that them in the control design;
- time step  $dt = 0.03$ ;
- center refinement for  $y$  mesh and no refinement for  $x$  mesh.

For the temporal scheme, we use Adam-Bashforth in order 3.

# Results

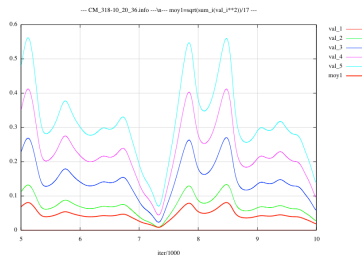


Figure 6: Values of the errors ( $\psi_m - \psi_d$ ) in the middle ( $L_x/2$ ) along  $y$ -axis.

- the desired state is such that:
 
$$\psi_d(y) = \int_{y_{min}}^y \left( \left( \frac{U_2 - U_1}{U_2 + U_1} \right) \frac{\tanh(hr)}{\tanh(h)} + 1 \right) dr;$$
- the desired state varies between 0 and 384.

# Outline

- 1 Introduction
- 2 The choice of the control
- 3 The modelling
- 4 The First results
- 5 Conclusion**

# Conclusion

## Summary

- design of a linearized state space model for the mixing-layer around a chosen state;
- design of a stabilizing control law for the linearized state space model;
- implementation of the control law in Incompact3D and first simulation are discussed.

## Perspectives

- concentrate more sites around the region of mixture: use a refined mesh for the design of the control law;
- take into account the disturbances on the control ( $P_u$ ): LQR-I? combine a feedforward and a feedback?

# Thank you for your attention!<sup>1</sup>

---

<sup>1</sup>Acknowledgments: thank you to Région Bretagne  for the financing of the project.

# References I

- D. Anda Ondo. *Modélisation et analyse des systèmes à paramètres distribués non linéaires par la méthode de Boltzmann sur réseau : application aux écoulements à surface libre*. These, Université de Grenoble, July 2013. URL <http://tel.archives-ouvertes.fr/tel-00860782>.
- K. Chatelain, A. Leroy, S. Aubrun, and J. Carlier. étude de la réceptivité d'un écoulement dynamique cisailé libre au forçage dynamique par actionneur plasma. 2013.
- X.-Q. Dao and C. Collewet. Drag Reduction of the Plane Poiseuille Flow by Partitioned Visual Servo Control. In *American control conference*, pages 4084–4089, Montréal, Canada, June 2012. URL <http://hal.inria.fr/hal-00726528>.
- T. Duriez, V. Parezanovic, B. R. Noack, and L. Cordier. Attractor control using machine learning, 2013. arXiv:1311.5250v1 [nlin.CD] 20 Nov 2013.
- . Gautier and J.-L. Aider. Feed-forward control of a perturbed backward-facing step flow. *J. Fluid Mech.*, 759:181–196, 2014. doi: 10.1017/jfm.2014.518.
- C.-M. Ho and L.-S. Huang. Subharmonics and vortex merging in mixing layers. *J. Fluid Mech.*, 119:443–473, 1982.



## References II

- C.-M. Ho and P. Huerre. Perturbed free shear layers. *Ann. Rev. Fluid Mech.*, 16: 365–424, 1984.
- M. M. Koochesfahani and C. G. MacKinnon. Influence of forcing on the composition of mixed fluid in a two-stream shear layer. *Phys. Fluids A*, 3(5):1135–1142, May 1991.
- S. Laizet and E. Lamballais. User guide incompact3d. Technical report, Université de Poitiers, 2011. Version 1.0.
- A. Michalke. On the inviscid instability of the hyperbolictangent velocity profile. *Journal of Fluid Mechanics*, 19:543–556, 8 1964. ISSN 1469-7645. doi: 10.1017/S0022112064000908. URL [http://journals.cambridge.org/article\\_S0022112064000908](http://journals.cambridge.org/article_S0022112064000908).
- J. McKernan. *Control of Plane Poiseuille Flow: A theoretical and Computational Investigation*. PhD thesis, Cranfield University, School of Engineering, 2006.
- D. Oster and I. Wygnanski. The forced mixing layer between parallel streams. *J. Fluid Mechanics*, 123:91–130, 1982.



## References III

- V. Parezanovic, T. Duriez, L. Cordier, B. R. Noack, J. Delville, J.-P. Bonnet, M. Segond, M. Abel, and S. L. Brunton. Closed-loop control of an experimental mixing-layer using machine learning control, 2014. Under consideration for publication in *J. Fluids Mech.*
- P. Roca, A. Cammilleri, T. Duriez, L. Mathelin, and G. Artana. Streakline-based closed-loop control of a bluff body flow. *Physics of Fluids*, 26, 2014. doi: 10.1063/1.487176.
- K. Sodjavi and J. Carlier. Experimental study of thermal mixing layer using variable temperature hot-wire anemometry. *Exp. Fluids*, 54, 2013. doi: 10.1007/s00348-013-1599-y.
- R. Tatsambon Fomena and C. Collewet. Fluid Flow Control: a Vision-Based Approach. *International Journal of Flow Control*, 3(2+3):133–169, Sept. 2011. URL <http://hal.inria.fr/hal-00701080>.
- J. M. Wiltse and A. Glezer. The effect of closed-loop feedback control on scalar mixing in a plane shear layer. *Exp. Fluids*, 51:1291–1314, 2011.
- I. Wygnanski and H. E. Fiedler. The two-dimensional mixing regions. *J. Fluids Mech.*, 41:327–361, 1970. part 2.